POLITECNICO DI TORINO
Repository ISTITUZIONALE

Bioinspired Fano-like resonant transmission: frequency selective impedance matching

Original
Bioinspired Fano-like resonant transmission: frequency selective impedance matching / Esposito, A., Tallarico, D., Sayed, A., Miniaci, M., Shahab, S., Bergamini, A.. - In: JOURNAL OF PHYSICS D. APPLIED PHYSICS. - ISSN 0022-3727. - 57:(2024), pp. 1-10. [10.1088/1361-6463/ad1c86]

Availability:
This version is available at: 11583/3009254 since: 2026-03-26T11:39:29Z

Publisher:
Institute of Physics

Published
DOI:10.1088/1361-6463/ad1c86

Terms of use:

This article is made available under terms and conditions as specified in the corresponding bibliographic description in the repository

Publisher copyright

(Article begins on next page)

09 September 2026

Journal of Physics D: Applied Physics

PAPER · **OPEN ACCESS**

Bioinspired Fano-like resonant transmission: frequency selective impedance matching

To cite this article: Andrea Esposito *et al* 2024 *J. Phys. D: Appl. Phys.* **57** 155402

View the article online for updates and enhancements.

You may also like

- Statistical RTA simulations of atomic data for astrophysical opacity modeling in the context of kilonova emission
Helena Carvajal Gallego, Jean-Christophe Pain, Michel Godefroid et al.
- Mechanistic modelling of relative biological effectiveness of carbon ion beams and comparison withexperiments
Haonan Feng, Weiguang Li, Yibao Zhang et al.
- Nonlinear corrections for the nuclear gluon distribution in eA processes
G.R. Boroun, Bita Rezaei and Fariba Abdi

This content was downloaded from IP address 38.68.237.144 on 30/01/2024 at 14:54

OPEN ACCESS
IOP Publishing
Journal of Physics D: Applied Physics
J. Phys. D: Appl. Phys. **57** (2024) 155402 (9pp)
https://doi.org/10.1088/1361-6463/ad1c86

Bioinspired Fano-like resonant transmission: frequency selective impedance matching

Andrea Esposito[1], Domenico Tallarico[1], Moustafa Sayed Ahmed[2], Marco Miniaci[3], Shima Shahab[2] and Andrea Bergamini[1,]

[1] Empa, Materials Science and Technology, Ueberlandstrasse 129, CH 8600 Duebendorf, Switzerland
[2] Department of Mechanical Engineering, Virginia Tech, Blacksburg, VA 24061, United States of America
[3] Univ. Lille, CNRS, Centrale Lille, Junia, Univ. Polytechnique Hauts-de-France, UMR 8520—IEMN—Institut d'Electronique de Microélectronique et de Nanotechnologie, F-59000 Lille, France

E-mail: andrea.bergamini@empa.ch

Received 4 October 2023, revised 8 December 2023
Accepted for publication 9 January 2024
Published 24 January 2024

Abstract

The study of the impedance mismatch between the device and its surroundings is crucial when building an acoustic device to obtain optimal performance. In reality, a high impedance mismatch would prohibit energy from being transmitted over the interface, limiting the amount of energy that the device could treat. In general, this is solved by using acoustic impedance matching layers, such as gradients, similar to what is done in optical coatings. The simplest form of such a gradient can be considered as an intermediate layer with certain qualities resting between the two media to impedance match, and requiring a minimum thickness of at least one quarter wavelength of the lowest frequency under consideration. The desired combination(s) of the (limited) available elastic characteristics and densities has traditionally determined material selection. Nature, which is likewise limited by the use of a limited number of materials in the construction of biological structures, demonstrates a distinct approach in which the design space is swept by modifying certain geometrical and/or material parameters. The middle ear of mammals and the lateral line of fishes are both instances of this method, with the latter already incorporating an architecture of distributed impedance matched underwater layers. In this paper, we develop a resonant mechanism whose properties can be modified to give impedance matching at different frequencies by adjusting a small set of geometrical parameters. The mechanism in question, like the lateral line organ, is intended to serve as the foundation for the creation of an impedance matching meta-surface. A computational study and parameter optimization show that it can match the impedance of water and air in a deeply sub-wavelength zone.

Keywords: biomimetics, acoustic matching layer, impedance, transmission, Fano-like resonance, impedance matching

Author to whom any correspondence should be addressed.

Original Content from this work may be used under the terms of the Creative Commons Attribution 4.0 licence. Any further distribution of this work must maintain attribution to the author(s) and the title of the work, journal citation and DOI.

© 2024 The Author(s). Published by IOP Publishing Ltd

1. Introduction

The study of impedance mismatch between materials/structures with varied properties (real or effective) is critical in acoustics to identify the overall behavior of the ensemble acoustic device/surrounds. Indeed, a significant impedance mismatch would prohibit energy from being transmitted over the interface, limiting the amount of energy that the device could treat. A common solution to this problem is to create an acoustic impedance matching layer with attributes that lie between the two impedance matching media. When combining materials with traditional elastic characteristics and densities, a minimum thickness of the order of one quarter wavelength of the lowest frequency under consideration is necessary in most circumstances [18].

Nature, which frequently deals with impedance matching problems in various fields of physics (from electromagnetism to mechanics and acoustics), is a valuable source of inspiration in this context (see figure 1) to this challenge, having optimized the space during eons of evolution through a sweep of geometrical and/or material characteristics. The middle ear of mammals and the lateral line of fishes are both clear instances of this method, with the latter already incorporating an architecture of distributed impedance matched underwater layers.

In this context, our work is inspired by animals' ability to detect acoustic waves, which is critical to their survival in their hunt for prey, to avoid becoming prey to other animals higher up the food chain, and as part of their reproductive activity [12]. The fundamentals of this function, from a physical standpoint, entail many transduction steps, including mechanical energy transmission over interfaces with high impedance mismatches. The most noteworthy example is the impedance mismatch between air and biological tissues (which have impedances of 1.4–1.8 MRayl and 0.004 MRayl, respectively). The literature has a diverse corpus of study on the impedance matching function of the middle ear, spanning from fundamental [35], to behavior of terrestrial animals [23, 24], and medical research [30]. Fish are also excellent candidates for addressing this issue since they have organs that detect mechanical vibrations in their surroundings. A number of canals in the head offer part of the information needed for survival in most of them, while an extra organ is disseminated over a bigger percentage of their bodies. The lateral line is the name given to this additional organ (see figure 1). This topic has a large corpus of study dedicated to it, both anatomically, physiologically, and ethologically [4, 8, 16, 25].

The neuromasts, which consist of a number of cilia protected by a thin membrane (cupula) and exposed to the flow of water surrounding the fish, are where signals are converted from mechanical waves to electrical polarization of cell membranes. Some of these neuromasts may be found on the fish's surface, exposed to free field fluid, while others are found within the lateral line canal. Figure 1 shows a schematic representation of the most typical geometry).

The 3D geometry of the lateral line canal deviates from the classical model given in figure 1 and in most ichthyology textbooks [34], according to a recent study of this organ in multiple species. There is agreement, however, that the scales are placed in a cantilever pattern, with the rostral extremities embedded in the fish's body and the caudal extremities free. The lateral line canal runs through pores in the scales and may have orifices for fluid exchange with the surrounding water. Neuromasts are found in the canal between the scales, as illustrated in figure 1. The canal neuromasts are stimulated by the flow of fluid within the canal, which is stimulated by the surrounding acoustic waves.

On the other hand, there is not much research on comparing the canal's impedance to the free field [9]. Despite the fact that the fluid within the lateral line canal and the environment surrounding the fishes are the same, there is agreement that the geometry of the canal impacts its impedance and makes it frequency dependent. Indeed, as is well known for brass instruments, available technical literature shows the importance of impedance mismatch at the terminations of cylindrical ducts [31].

We propose that the coupling of acoustic power into the lateral line canal is strongly influenced by the input impedance at the canal orifices, and that auxiliary mechanisms (such as cantilevered scales and their mechanical action on the fluid in the canal) are used to overcome impedance barriers and improve the coupling of incoming free field waves into the canal. A study of available literature, however, could neither expressly support nor disprove this notion.

Bridging acoustic impedance mismatch at interfaces is a technical problem that is typically addressed by employing one or more impedance matching layers [27], made of suitable materials with impedance values falling between the semi-spaces to be connected [3]. Wave absorption, sensing, energy transfer, and harvesting are obvious applications where impedance matching is critical.

Mechanical metamaterials (structured fluid or solid media) enable the fabrication and control of novel acoustic functions that would otherwise be unavailable in regular homogeneous media. Acoustic cloaking, focusing, absorption, and noise reduction are examples of these [19]. Furthermore, due to its potential to produce matching between fluid media with differing acoustic impedance, anomalous transmission of acoustic energy through narrow (relative to the wavelength of the incoming acoustic wave) surface-like meta-structures is gaining interest. Perhaps the most convincing example is the air-water interface, which covers 70% of the earth's surface and has a three order of magnitude impedance mismatch. Metamaterial-based solutions based on gradient metagels [10] enable nearly-total broadband transmission for modest (same order of magnitude) impedance mismatch. The utilization of resonant effects becomes physically unavoidable as the mismatch becomes more extreme [2]. This resonant effect is often used in ultrasound power transfer devices to maximize transmission [1, 28, 29]. Indeed, sub-wavelength Helmholtz-like resonators comprised of a closed volume of fluid combined with a resonant membrane ensure nearly entire absorption [22] or transmission through the water-air [5]. Another technique for artificially equalizing the air-water impedance is the employment of bubbles, notably the sub-wavelength

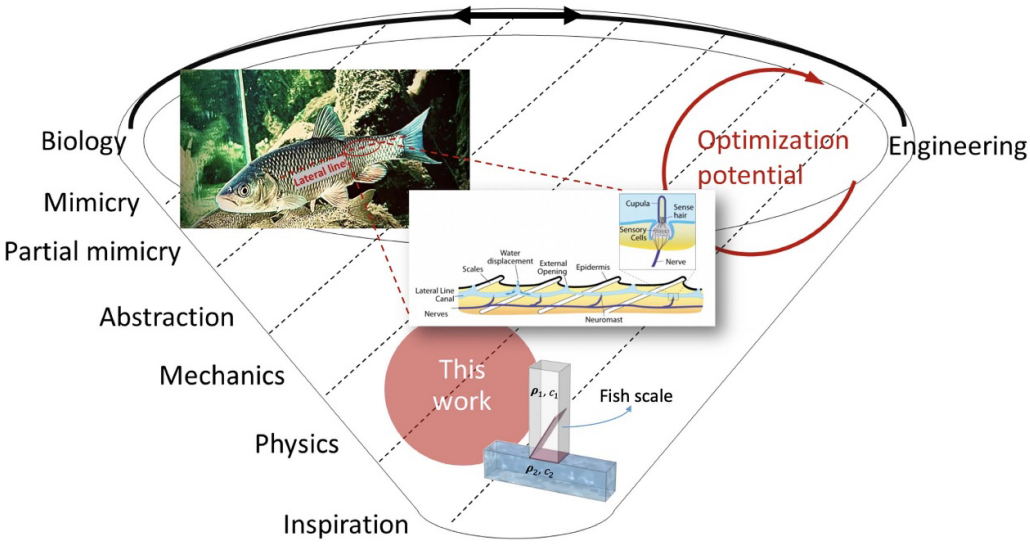

Figure 1. A representation of different levels of bio-mimicry and bio-inspiration, from the observation of biological systems to the development of engineering structures, position of the present work, and the proposed unit-cell for Fano-like resonant transmission between two acoustic media with densities $_1$ and $_2$ and sound velocities c_1 and c_2. The figure includes a schematic representation of the lateral line organ (frontal section [13]), showing the canal in which neuromasts are located, in between scales. The lateral line canal goes across scales through orifices present in each of them. Pores allow for the exchange of fluid with the environment. The figure is adapted from [32].

nature of their modes of vibration, which enables ultra-low frequency applications to be targeted [6]. Controlling bubble location and formation has been improved by 'sculpturing' air cavities just below the water-air interface using hydrophobic lightweight meta-material scaffolds [7, 14] A new bio-inspired concept that takes advantage of the hydrophobic properties of lotus leaves has just been proposed [15]. Aside from matching the impedance (thus increasing transmission), the metasurface may also operate as a 'lens,' aiding the focussing of acoustic radiation for more effective long-distance communication. In this regard, coiled-up space metamaterial surfaces [20] have recently permitted remote simultaneous impedance matching and focusing (by inhomogeneous by-design phase delay).

In this study, we describe a resonant element with the ability to bridge the impedance mismatch between two acoustic media with highly different properties, inspired by the fish scales of the lateral line organ. To allow energy transmission over the interface, we created air and water semispaces with densities of $\rho_1 = 1.2\,\mathrm{kg\,m}^{-3}$ and $\rho_2 = 1000\,\mathrm{kg\,m}^{-3}$, and speeds of sound $c_1 = 434\,\mathrm{m\,s}^{-1}$ and $c_2 = 1480\,\mathrm{m\,s}^{-1}$, respectively. We argue that, in the meaning of figure 1, the design should be deemed bio-inspired because it is informed by a good grasp of mechanisms that govern the operation of the lateral line organ as provided by the existing body of literature. The device has a far simpler design than the mammal middle ear and exhibits Fano-like resonance activity. Fano resonances are common in quantum mechanics [11] and classical [17] systems alike: A resonant asymmetric transmission as a function of frequency occurs whenever a background scattering process (here understood as the transmission of sound waves at the air-/water interface) interferes with a system sustaining a discrete spectrum (here embodied by the eigenmodes of the fish scale) (*cf* figure 5).

In future applications, the proposed novel vibroacoustic element could be a unit cell of an impedance matching meta-surface. The reason for using a bio-mimetic approach to the construction of impedance matching layers is clearly stated in [33]: Nature's method of substituting structure (i.e. some kind of information) for materials requiring high energy processes for synthesis has benefits for engineering applications as well. Here, the increased material flexibility offered by the meso-level supplemental layer of architecture provides for additional requirements such as environmental, economical, or functional.

2. Unit cell analysis and methodoloy to design Fano-like resonant transmission mechanism

The main equations determining energy flow in linear lossless acoustic medium are summarized here. Time-harmonic pressure waves $P(\mathbf{r},t) = p(\mathbf{r})e^{\ i\ t}$ in an acoustic lossless channel are governed by the Helmholtz equation

$$\nabla^2 p(\mathbf{r}) \quad k^2 p(\mathbf{r}) = 0. \tag{1}$$

If we assume that

1. the particle velocity

$$\mathbf{v}(\mathbf{r}) = \frac{i}{\rho\omega}\nabla p(\mathbf{r}), \tag{2}$$

vanishes, in the normal direction to the boundary walls;
2. the interface between the two fluids is flat;

then we can calculate the pressure on either sides of the interface independently of the x and y coordinates. In such a

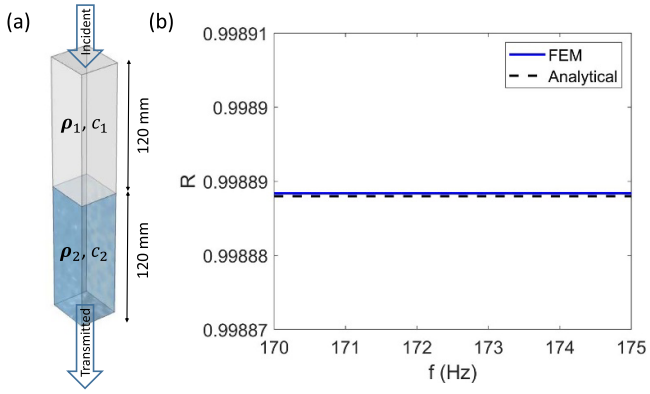

Figure 2. (a) The system diagram of two distinct acoustic mediums in contact. (b) The reflection coefficient at the water–air interface was estimated numerically using FEM and confirmed by the analytical relationship in equation (7).

circumstance, solutions to equation (1) are written in the plane-wave form. Wave scattering at an impedance mismatched interface between two semi-infinite columns of fluid within a channel reduces to wave scattering from a mismatch between two semi-infinite spaces, a well-known 1D problem. Indeed, with reference to figure 2(a), if we assume that the fluid interface lays at $z = 0$, the equilibrium and compatibility conditions are satisfied by

$$\begin{aligned} p(z) &= p_0 \exp(i\omega z/c_1) \\ &\quad + \mathcal{R}\exp(\quad i\omega z/c_1), \\ &\quad \text{for } z < 0, \\ &\text{and} \\ p(z) &= \mathcal{T}\exp(i\omega z/c_2), \\ &\quad \text{for } z > 0 \end{aligned} \tag{3}$$

with

$$\mathcal{R} = \frac{\quad_2 \quad _1}{\quad_2 + \quad_1} p_0, \quad \text{and} \quad \mathcal{T} = \frac{2\ \quad_2}{\quad_1 + \quad_2} p_0. \tag{4}$$

where we have introduced the acoustic impedance $\quad_1 = \rho_1 c_1$ and $\quad_2 = \rho_2 c_2$, and p_0 is the incident wave pressure amplitude.

The acoustic power [26] associated with a pressure wavefield $p(\mathbf{r}, t)$ flowing through a cross-section $\quad$, with normal vector $\mathbf{n}$ perpendicular to z, is

$$P = \frac{1}{2} \quad \mathrm{d}^2\mathbf{n} \cdot \mathrm{Re}(p\mathbf{v}^*), \tag{5}$$

where $(\cdot)^*$ denotes complex conjugation. We can choose the incidence pressure amplitude without losing generality in order to acquire unit incident power, i.e. the cross-sectional area.

By employing the sound pressure field equations (3) in (2), with coefficient as in equation (4), and assuming unit incident power (i.e. $p_0 = \sqrt{2\ \ _1/S}$), the acoustic power (5) through cross-sections in the 1- and 2- material yield

$$P_1 = 1 \quad R, \quad \text{and} \quad P_2 = T, \tag{6}$$

respectively, where

$$R = \left(\frac{\quad_2 \quad _1}{\quad_2 + \quad_1}\right)^2, \quad \text{and} \quad T = \frac{4\ \quad_1\ \quad_2}{(\quad_2 + \quad_1)^2}. \tag{7}$$

We notice that the formulations for the scattered fluxes satisfy the conservation of power, i.e. $P_1 = P_2$ or $1 = R + T$. The transfer matrix method, for example, can be used to represent impedance matching layers analytically. This necessitates understanding of the effective mechanical properties of each layer. In the case of structured layers (metasurfaces), these must be explored using an equivalent model that must be developed. We chose a numerical approach for this purpose that allows us to first model the interface between the fluids, allowing the results to be easily verified analytically, based on (3), with conservation of scattered power as an indicator of the numerical model's quality. Similarly, simple models were created separately to investigate the dynamic behavior of the proposed structures in order to determine the effect of design parameters on structural response. These models can then be supplemented with the essential structural components and fluid-structure interactions to explain the proposed impedance-matching structure.

3. Physical mechanisms: from natural designs to optimized structures

We begin by investigating the transmission and reflection of energy at the interface of two fluids in contact. Using COMSOL Multiphysics, we created a finite element model (FEM) of a duct with an acoustic domain of air and one of water, as illustrated schematically in figure 2(a), and analytically, we validate the FEM scattered power predictions. A 2D frequency analysis model is employed to address the physics of the underlying acoustic-solid interaction problem. By assuming a free quadrilateral mesh, the study samples the pressure waves within the desired frequency range. To obtain accurate results, convergence of the two studies namely frequency analysis and eigenfrequency studies are performed at the fluid-structure interface to determine the appropriate mesh element size. Results converge at a mesh size of 0.125 mm, and this size was selected for the study. For an incoming planar pressure wave, we use equation (6) at the inlet surface to extract the reflected power. The channel's lateral sides are treated as acoustically hard walls, while the inlet and outlet surfaces are outfitted with radiation conditions to simulate the fluid columns' semi-infinite extension.

The acoustic power reflected and transmitted at the interface between the two fluids is then calculated. Figure 2(b) shows excellent agreement between the FEM prediction and the analytical value calculated from equation (7).

The bio-inspired resonant impedance matching element is then introduced to examine its effect on energy transmission across the interface. We developed a 2D solid geometry inspired by the fish scale design for this purpose and positioned it at the interface between the two fluids, as illustrated schematically in figure 3(a2). A detailed schematics with the attached

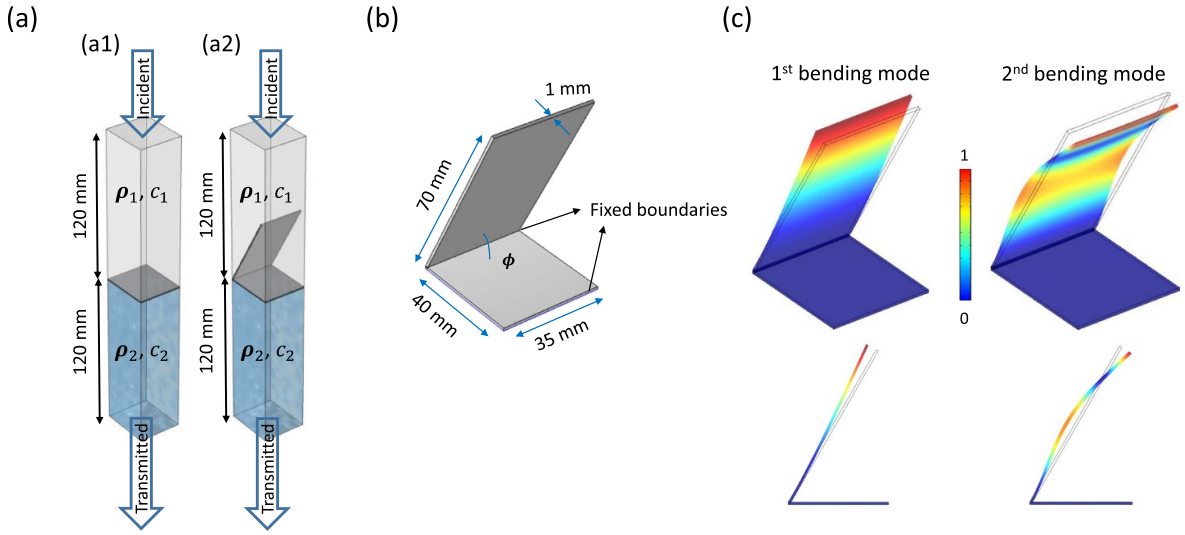

Figure 3. (a) The schematic of (a1) a flat plate and (a2) a fish scale separating air and water zones. (b) A comprehensive schematic of the fish scale utilized in this investigation, with dimensions attached. (c) A 3D FEM results of displacement profiles of the eigenfrequency analysis showing the 1st and 2nd bending mode shapes.

Table 1. Material properties of the fish scale.

Property	E (GPa)	(kg m ^{3})	ν	Q
Value	70	2700	0.33	5000

Table 2. Eigenfrequencies of the coupled structural-acoustics system.

Eigenmode	f [Hz]	type
1	172.1	1st bending mode
2	1069	2nd bending mode

dimensions is shown in figure 3(b). This scale depicts a hypothetical impedance-matching metasurface unit. The scale's base plate is 35×40 mm and 1 mm thick, with a long side of 70 mm. A fixed mechanical boundary condition is applied at the two bottom borders. In figure 3(c), a 3D FEM eigenfrequency analysis is developed to illustrate the bending mode shapes.

As shown in figure 3(a1), the scale's behavior is compared to that of a neat air-water interface and a simple flat plate of the same size as the base plate of the fish scale situated at the interface. The flat plate and fish scale mechanical properties are given in table 1 where ν and Q denote Poisson's ratio and the mechanical quality factor, respectively. The scale's mobility is projected to rise significantly in proximity of its eigenfrequencies. To determine the first two eigenfrequencies of the coupled system, we do a modal analysis. (see table 2 for the frequencies and figure 3(c) for the mode shapes). The remainder of this paper focuses on the impact of the first bending mode on mechanical power transmission across the air-water interface, as well as the frequency response of the system near the first bending mode.

The efficiency of the fish scale in improving the normal energy transmission between the two fluids is evident by referring to figure 4(a) showing the normalized acoustic power contributions for the two cases, air and water separated by a thin plate and separated by the fish scale. The fish scale implies a progressive increase in transmission until it reaches a maximum perfectly in line with the first bending mode, signifying maximum energy passed between the two fluids; above 172 Hz, the transmission abruptly decreases and returns to the flat plate value. The reflection in figure 4(a) on the other hand, exhibits a specularly opposite tendency, reaching a minimum value at the first eigenfrequency, indicating that the amount of reflected energy declines while the amount of transmitted energy grows. In fact, at the fish scale's resonance frequency (172 Hz), the reflected energy reduces by around 27.2 while the transmitted energy increases by 24.6 . The difference between the two percentages can be attributable to the energy lost (about 2.6) within the fish scale.

The dashed black curve in figure 4(a) shows this, with a minimum of 97.4 at the resonance frequency. As seen in figure 4(a), the fish scale exhibits a Fano-like resonance around the fish scale, with anti-resonance at roughly 176.7 Hz. Furthermore, figure 5 illustrates that the flat plate leads to lesser transmission when compared to direct contact between air and water. This is to be expected because the plate adds an impedance.

The deformation of the fish scale at the resonance frequency works as a mechanism for transferring energy from one medium to another. This is clearly seen in figure 6(c), which depicts the normalized vertical displacement amplitude of the face in contact with water (indicated in red in the attached schematic) for various scale angles. Finally, figure 4(b) depicts the power transferred by the fish scale normalized by the power transmitted by the flat plate. The bio-inspired structure clearly allows a transmission that is roughly 220 and 500 times

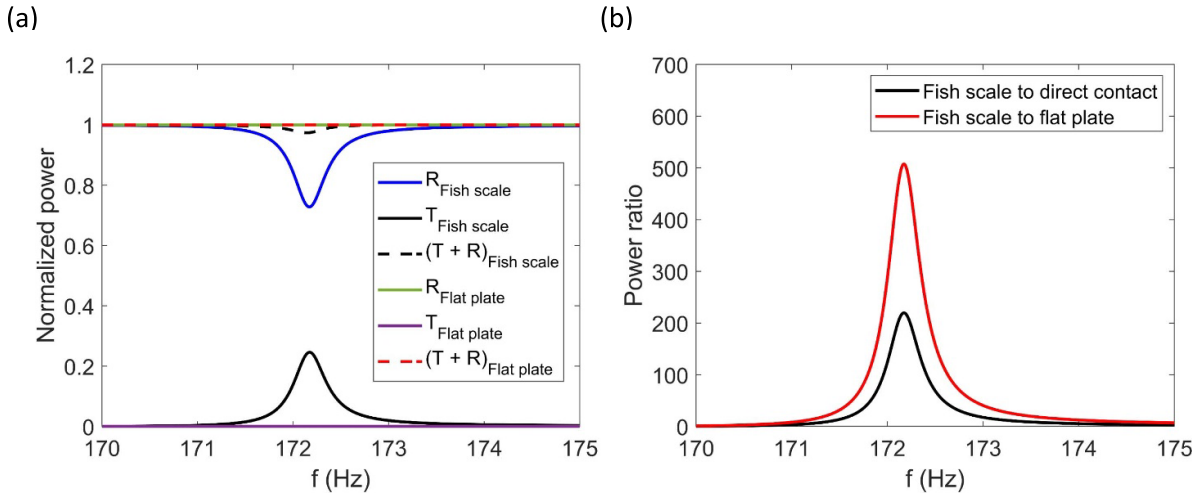

Figure 4. (a) Transmission and reflection coefficients at the air–water interface through the fish scale and flat plate near the fish scale's 1st bending mode and (b) the ratio of the transmitted power through the fish scale to the transmitted power through the flat plate.

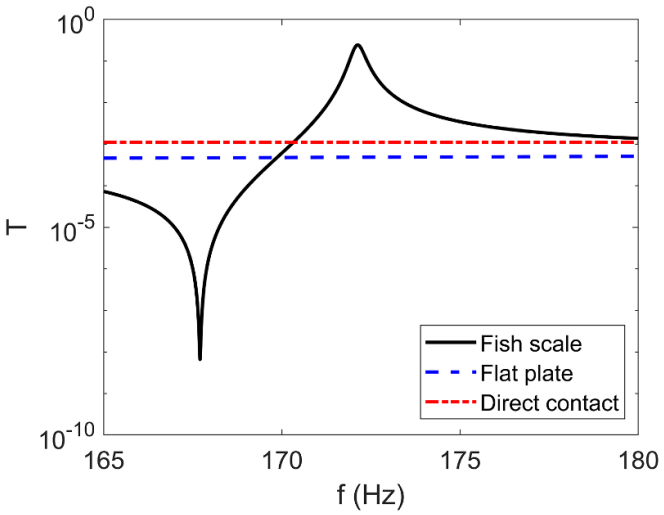

Figure 5. Transmission coefficient of the fish scale, flat plate and a direct contact between air and water.

more efficient than an air-water direct contact and a flat plate, respectively.

Several fish scale factors, such as their dimension and mechanical qualities, can influence the energy transfer of our system. The contour plot in figure 6(a) shows how variations in the angle of the fish scale, as well as changes in Young's modulus and density, affect the transmission coefficient. Consistently multiplying the material density by a fixed ratio of E/rho (values given in table 1) to derive the Young's modulus maintains a constant wave propagation speed and resonant frequency. It can be noted from figures 6(a) and (b) that the transmission coefficient is maximized for lower Young's modulus and scale angle values. This is because significant vertical deflection in the face in contact with water occurs at lower angles and lower Young's modulus values. This is depicted in figure 6(c) for four different scale angles while keeping E at 70 GPa and ρ at 2700 kg m ^{3} constant. For instance, the transmission of a system with a 70 mm upper plate length drops down from 24.3% to 8% when the angle is changed from $\phi = 60°$ to $\phi = 72°$ (see the red curve in figure 6(d)). This corresponds to maximum normalized vertical displacements of 1 and 0.55 respectively as shown in figure 6(c). The potential group of materials, which corresponds to the given values of Young's moduli and densities, is depicted on the left side of figure 6(a). The length of the upper plate of the fish scale is another parameter to be investigated. The transmission coefficient is determined in figure 6(d) by adjusting the scale angle for different scale lengths. All curves tend to converge toward a lower transmission value as the scale angle increases. As the scale angle increases, similar behavior is found for other material properties (see figure 6(a)). When considering a fixed angle, for $\phi < 70°$, better transmission is observed with longer lengths. However, when the lowest attainable angle for each length is examined, shorter lengths correspond to better transmission coefficients.

Finally, in the last test case, the air domain is linked to a horizontal water channel with double symmetric outlet bifurcations (figure 7(a)). These findings provide more evidence for the bioinspired structure's usefulness in enhancing coupling and hence energy transmission between two fluids. As previously stated, a simple separation plate does not permit energy transfer in the frequency regime under consideration, figure 7(b) shows the components of reflection and transmission coefficients for the fish scale only. The incoming transmitted power is divided equally between two channels heading to an outlet, the sum of which yields the overall transmission, which, as expected, is obtained at the scale's resonance frequency. This figure corresponds to about 28.7% of the incident power in the system. The final example shown here is closer to a feasible design and so serves as a foundation for future improvements in the coupling of sound energy from a gaseous medium into liquid-filled channels. Furthermore, instead of the complete symmetry depicted in figure 3(b), it

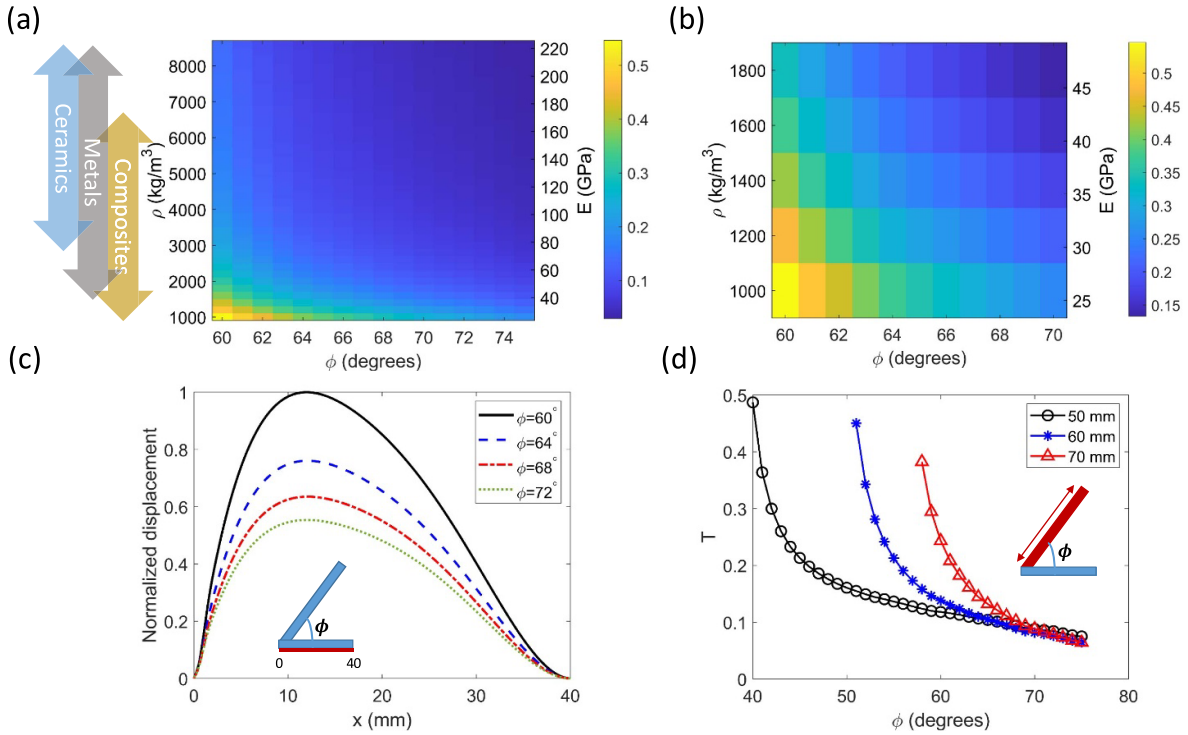

Figure 6. The effects of density, Young's modulus, and fish scale angle on the transmission coefficient of the system for various materials are shown in (a), and a zoomed plot encompassing the high-T area is shown in (b). (c) The vertical displacement magnitude of the lower edge of the fish scale (highlighted in red) for various scale angles. (d) The transmission coefficient fluctuation for varied upper plate length values for fish scales (highlighted in red).

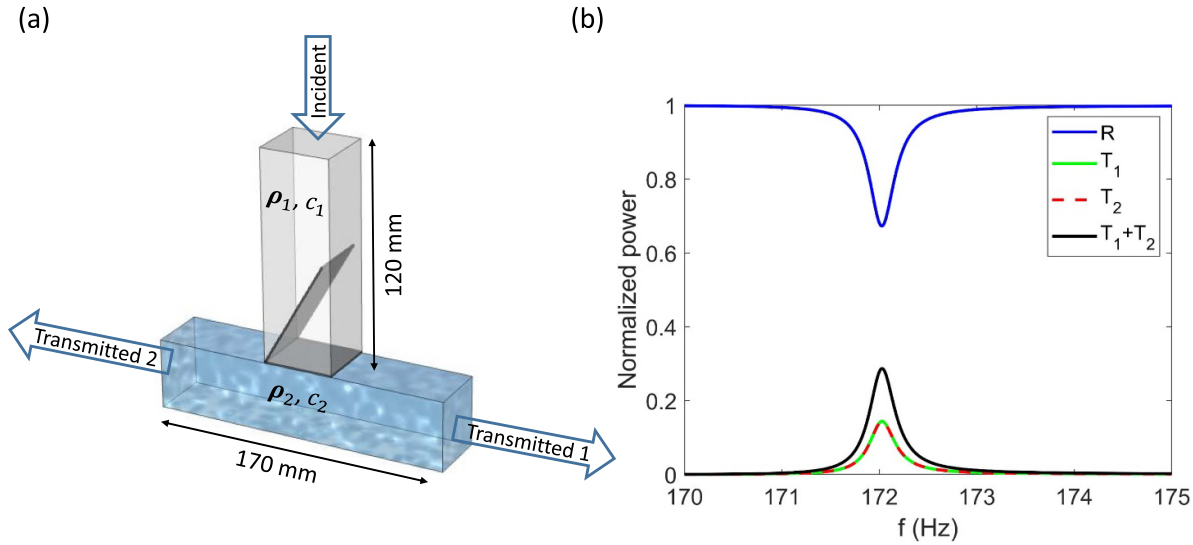

Figure 7. (a) A schematic of a power transmission system through the fish scale consisting of two outlets. (b) FEM results of the transmission and reflection coefficients at the air–water interface through the fish scale. Here T_1 and T_2 correspond to the transmitted normalized power for outlet 1 and 2 shown in (a).

may be advantageous to investigate its orientation with regard to the channel in order to achieve a preferable direction of transmission.

The simplicity of the geometry of the device shown in figure 4 is expected to facilitate the planned experimental verification of the work carried out so far as well as a key to a future implementation in real resonant meta-interfaces. A physical implementation of this concept for verification purposes can be envisaged by 3D-printing a fish-scale. This would allow to easily manufacture the necessary extensions to the plate in the plane of the air–water interface, to clamp either end of the device to a purpose-built impedance tube. The materials and dimensions of the impedance matching device are such that conventional selective laser melting processes would be

a viable production method. Alternatively, laser cutting and machine bending of thin aluminum plates is a method of manufacturing closer to industrial fabrication of meta-interfaces. The up-scaling of this concept implies the preparation of arrays of fish scales to cover large surfaces. For this purpose, it would be possible to extrude appropriate profiles and post-process them to produce impedance matching layers on a bigger scale.

4. Conclusions

As in locally resonant metamaterials [21], the mechanism reported in this paper can interact with incoming acoustic waves despite its significantly sub-wavelength dimensions due to a substantial drop in the mechanical impedance of the system during resonance. If we regard the length of the scale ℓ as the characteristic length of the system, the ratio between the fish scale characteristic size and the length of the wave at its resonant frequency is about 1/30. The impedance matching function, like that of sense organs such as the lateral line or the ear, is implemented by a conceptually simple mechanism, eventually a lever.

Targeted frequencies are proven in this work to be better communicated between them when a resonant interface element is used rather than a clean interface between the media. When applied in the context of a meta-surface (or, more accurately, a meta-interface) between two media, such elements are projected to significantly increase energy transmission between the media. A rainbow technique, which employs a variety of resonant frequencies, will provide broad band behavior.

According to a bio-mimetic method, the geometry of the fish-scale unit can be tuned based on the needs and frequencies of interest, as well as the material used to make it. This use of geometry ('information' as defined [33]) as the prominent parameter of the meta-surface's unit cell to obtain a specific set of properties contrasts with the common approach, which involves the selection of materials ('energy' [33]) to achieve a specific function. This allows for the implementation of a wide range of attributes based on a small number of different material classes, as observed in Nature. Technically, this paradigm shift toward the use of geometry over the selection of materials with specific properties (in this case, a range or gradient of acoustic impedance values) means more freedom in material selection to meet other constraints such as cost, sustainability, or application-specific requirements such as strength, corrosion resistance, or electromagnetic properties.

Data availability statement

The data that support the findings of this study are openly available at the following URL/DOI: https://zenodo.org/communities/boheme/.

Acknowledgments

A E, M M, and A B received funding from the European Union's Horizon 2020 research and innovation programme under Grant Agreement No. 863179. M S A and S S gratefully acknowledge support from US National Science Foundation (NSF) under Grant Nos. ECCS-171113 and CMMI-CAREER 2143788. All the Authors declare not to have any financial or otherwise competing interest related to the published work.

ORCID iDs

Domenico Tallarico https://orcid.org/0000-0001-5980-8950
Moustafa Sayed Ahmed https://orcid.org/0000-0002-4668-1855
Marco Miniaci https://orcid.org/0000-0002-6830-3548
Shima Shahab https://orcid.org/0000-0003-1970-5345
Andrea Bergamini https://orcid.org/0000-0003-2722-3207

References

[1] Ahmed M A S, Robert B, Ghommem M and Shahab S 2022 Genetic algorithm optimization for through-wall ultrasound power transfer systems *Active and Passive Smart Structures and Integrated Systems XVI* (SPIE)
[2] Alvarez-Arenas T G 2004 Acoustic impedance matching of piezoelectric transducers to the air *IEEE Trans. Ultrason. Ferroelectr. Freq. Control* **51** 624–33
[3] Bakhtiari-Nejad M, Hajj M R and Shahab S 2020 Dynamics of acoustic impedance matching layers in contactless ultrasonic power transfer systems *Smart Mater. Struct.* **29** 035037
[4] Bleckmann H and Zelick R 2009 Lateral line system of fish *Integr. Zool.* **4** 13–25
[5] Bok E, Park J J, Choi H, Han C K, Wright O B and Lee S H 2018 Metasurface for water-to-air sound transmission *Phys. Rev. Lett.* **12** 044302
[6] Bretagne A, Tourin A and Leroy V 2011 Enhanced and reduced transmission of acoustic waves with bubble meta-screens *Appl. Phys. Lett.* **99** 221906
[7] Cai Z, Zhao S, Huang Z, Li Z, Su M, Zhang Z, Zhao Z, Hu X, Wang Y-S and Song Y 2019 Bubble architectures for locally resonant acoustic metamaterials *Adv. Funct. Mater.* **29** 1906984
[8] Coombs S, Bleckmann H, Fay R R and Popper A N 2014 *The Lateral Line System* (Springer)
[9] Denton E J and Gray J A B 2012 *Sensory Biology of Aquatic Animals* (Springer) ch 23, pp 595–617
[10] Dong E, Song Z, Zhang Y, Mosanenzadeh S G, He Q, Zhao X and Fang N X 2020 Bioinspired metagel with broadband tunable impedance matching *Sci. Adv.* **6** eabb3641
[11] Fano U 1961 Effects of configuration interaction on intensities and phase shifts *Phys. Rev.* **124** 1866
[12] Fay D B W R R and Popper A N 1992 The evolutionary biology of hearing
[13] Haslwanter T 2012 Lateralline organ.jpg (Wikimedia Commons) (available at: https://commons.wikimedia.org/wiki/File:LateralLine_Organ.jpg)

[14] Huang Z *et al* 2021 Tunable fluid-type metasurface for wide-angle and multifrequency water-air acoustic transmission *Research* **2021** 9757943
[15] Huang Z *et al* 2021 Lotus metasurface for wide-angle intermediate-frequency water–air acoustic transmission *ACS Appl. Mater. Interfaces* **13** 53242–51
[16] Kasumyan A 2003 The lateral line in fish: structure, function and role in behavior *J. Ichthyol.* **43** S175
[17] Khanikaev A B, Wu C and Shvets G 2013 Fano-resonant metamaterials and their applications *Nanophotonics* **2** 247–64
[18] Krečka J, Čepl O and Habán V 2022 Quarter wavelength resonator in experiment and simulation *EPJ Web Conf.* **269** 01030
[19] Liao G, Luan C, Wang Z, Liu J, Yao X and Fu J 2021 Acoustic metamaterials: a review of theories, structures, fabrication approaches and applications *Adv. Mater. Technol.* **6** 2000787
[20] Liu J, Li Z, Liang B, Cheng J-C and Alu A 2023 Remote water-to-air eavesdropping with a phase-engineered impedance matching metasurface *Adv. Mater.* **35** 2301799
[21] Liu Z, Zhang X, Mao Y, Zhu Y, Yang Z, Chan C and Sheng P 2000 Locally resonant sonic materials *Science* **289** 1734–6
[22] Ma G, Yang M, Xiao S, Yang Z and Sheng P 2014 Acoustic metasurface with hybrid resonances *Nat. Mater.* **13** 873–8
[23] Mason M J 2016 Structure and function of the mammalian middle ear. I: large middle ears in small desert mammals *J. Anat.* **228** 284–99
[24] Mason M J 2016 Structure and function of the mammalian middle ear. II: inferring function from structure *J. Anat.* **228** 300–12
[25] Montgomery J, Bleckmann H and Coombs S 2014 Sensory ecology and neuroethology of the lateral line *The Lateral Line System* ed S Coombs, H Bleckmann, R R Fay and A N Popper (Springer) pp 121–50
[26] Pierce A D 2019 *Acoustics: An Introduction to Its Physical Principles and Applications* (Springer)
[27] Rathod V T 2020 A review of acoustic impedance matching techniques for piezoelectric sensors and transducers *Sensors* **20** 4051
[28] Sayed A, Ghommem M and Shahab S 2022 Mode couplings in multiplex electromechanical structures *J. Appl. Phys.* **132** 124901
[29] Sayed A and Shahab S 2023 Electrode pattern definition in ultrasound power transfer systems *Appl. Phys. Lett.* **122** 124101
[30] Schär M, Dobrev I, Röösli C, Huber A M and Sim J H 2023 Effects of preloads on middle-ear transfer function and acoustic reflex in ossiculoplasty with PORP *Hear. Res.* **430** 108709
[31] Smyth T and Abel J S 2009 Estimating waveguide model elements from acoustic tube measurements *Acta Acust. United Acust.* **95** 1093–103
[32] Vincent J F 2001 Stealing ideas from nature *Deployable Struct.* **412** 51–58
[33] Vincent J F 2008 Biomimetic materials *J. Mater. Res.* **23** 3140–7
[34] Webb J F and Ramsay J B 2017 New interpretation of the 3-D configuration of lateral line scales and the lateral line canal contained within them *Copeia* **105** 339–47
[35] Zwislocki J 1962 Analysis of the middle-ear function. part I: input impedance *J. Acoust. Soc. Am.* **34** 1514–23